DBEM analysis for an elliptic torsion bar with a double-edge crack

Yu Fan[1], Ying-Te Lee[1], Jia-Wei Lee[1] and Jeng-Tzong Chen[1, 2]

[1]Department of Harbor and River Engineering
National Taiwan Ocean University
[2]Department of Mechanical and Mechatronic Engineering
National Taiwan Ocean University
19952064@ntou.edu.tw

NSC Project: NSC 100-2221-E-019-040-MY3

ABSTRACT

It is well known that rank deficiency occurs in BEM for degenerate boundary. The conventional BEM is difficult to solve the problem which contains degenerate boundary without decomposing the domain to multi-regions. Therefore, the hypersingular integral equation is used to ensure a unique solution for the problem containing a degenerate boundary. By combining the singular and hypersingular equations it's termed dual BEM due to its dual frame. By employing the SVD technique to the four influence matrices, it is interesting to find that true information in physics due to rigid body mode is found in the right unitary vector with respect to the corresponding zero singular value while the degenerate boundary information in mathematics is imbedded in the left unitary vector. In this paper, we use the dual BEM to determine the torsional rigidity of an elliptic bar containing a double-edge crack. The role of the right and left unitary vectors of SVD in the dual BEM is also discussed in this work.

Keywords: degenerate boundary, dual BEM, null-field integral equation, SVD, torsional rigidity.

1. INTRODUCTION

In 1956, Kinoshita and Mura [1] derived the singular boundary integral equation for elasticity. Later, the boundary element method (BEM), or sometimes called boundary integral equation method (BIEM), has been used efficiently since Rizzo [2] discretized the integral equation for elastostatics in 1967. Over twenty years, the main applications were limited in boundary value problems (BVPs) without degenerate boundary, because the degenerate boundary caused the rank deficiency of influence matrices ([*U*] and [*T*]) in the conventional BEM. Traditionally, the multi-domain BEM was presented to solve the nonunique solution by employing an artificial boundary in the two decades (1960-1988). In other words, we must decompose the domain to sub-domains for solving this kind of problems [3] However, the main spirit and merit of BEM is that we only need to deal with the real boundary of the problem.

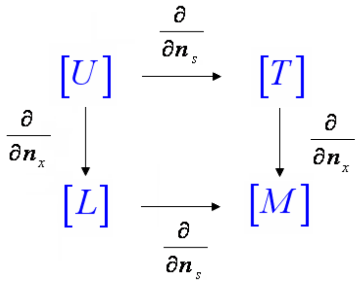

Figure 1 The dual frame of [*U*]、[*T*]、[*L*] and [*M*]

Obviously, domain decomposition of problems has disobeyed the main object.

In order to solve the problems containing a degenerate boundary (e.g., crack problems [3-8], sheet pile problems [9-11] and thin airfoil problems [12-14]) directly, Hong and Chen [16] presented the dual boundary integral equations to solve fracture mechanic problems. This dual system incorporates the displacement and traction boundary integral equations. The dual integral formulations have been applied successfully. By introducing the hypersingular equation, the influence matrices ([*U*]、[*T*] and [*L*]、[*M*]) have a dual framework as shown in Fig. 1. By using the dual integral formulation, even the problem containing degenerate boundary can be solved efficiently in a single domain. It was not necessary to decompose the domain anymore by discretizing the boundary of domain.

Torsion problems of a circular bar with a single edge crack [16, 17], a circular bar with circular holes/inclusions [18, 19] or an elliptic bar with elliptic holes/ inclusions [20] had been solved in the past. Mi and Aliabadi [21] even extended two-dimensional cases to three-dimensional crack problems. But they did not discuss the phenomenon of physics and mathematics in the dual BEM to the authors' best knowledge.

By employing singular value decomposition technique [22] with respect to the four influence matrices ([*U*]、[*T*]、[*L*]and[*M*]) in the dual BEM, the roles in the right and left unitary vectors are examined. It is interesting to discuss the unitary vectors correspond zero singular value. Degenerate boundary and rigid-body

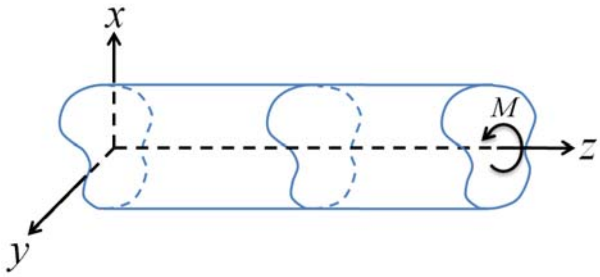

Figure 2 A torsion bar with a noncircular cross

contributes the zero singular value in the four influence matrices mathematically and physically. It was discovered that the true information in physics due to rigid-body mode is found in the right unitary vector, and the spurious information in mathematics is imbedded in the left unitary vector due to the degenerate boundary.

In this paper, the dual boundary element method is employed to solve a torsion problem of an elliptic bar containing a double-edge crack. We use the dual BEM to determine the torsional rigidity. Rank-deficiency of the four influence matrices was studied by using the SVD technique. Several examples will be given in this paper. Our results are compared with analytical solution derived by Lebedev et.al. [23]. Besides, we supply the constraint by putting the collocation point outside the domain (null-field point) to solve the torsion problem and to determine the torsional rigidity. Finally, the role in the right and left unitary vectors correspond to the zero singular value of SVD is also discussed in this article.

2. FORMULATION OF THE TORSION PROBLEM

2.1 Derivation of torsion function

The torsion problem of a bar with arbitrary cross is considered as depicted in Fig. 2. Following the theory of Saint-Venant torsion [24], we assume the displacement field (*u*, *v*, *w*) in the form

$$u=-\alpha yz,\qquad v=\alpha xz,\qquad w=\alpha\phi(x,y),\tag{1}$$

where (*x*, *y*, *z*) denote Cartesian coordinates, α is angle of twist per unit length along the *z*-axis and $\phi(x,y)$ is the warping function. The relationship between the displacement field and the strain components is as follows

$$\begin{aligned}&\varepsilon_x=\frac{\partial u}{\partial x},\qquad \varepsilon_y=\frac{\partial v}{\partial y},\qquad \varepsilon_z=\frac{\partial w}{\partial z},\\&\gamma_{xy}=\frac{\partial u}{\partial y}+\frac{\partial v}{\partial x},\quad \gamma_{yz}=\frac{\partial v}{\partial z}+\frac{\partial w}{\partial y},\quad \gamma_{zx}=\frac{\partial w}{\partial x}+\frac{\partial u}{\partial z}.\end{aligned}\tag{2}$$

By substituting Eq.(1) into Eq.(2), we can derive the strain components as

$$\begin{aligned}&\varepsilon_x=\varepsilon_y=\varepsilon_z=\gamma_{xy}=0,\\&\gamma_{yz}=\alpha\left(\frac{\partial\phi(x,y)}{\partial y}+x\right),\quad \gamma_{zx}=\alpha\left(\frac{\partial\phi(x,y)}{\partial x}-y\right),\end{aligned}\tag{3}$$

and the stress components can be obtained by applying Hooke's law as follows

$$\begin{aligned}&\sigma_x=\sigma_y=\sigma_z=\tau_{xy}=0,\\&\tau_{yz}=G\alpha\left(\frac{\partial\phi(x,y)}{\partial y}+x\right),\quad \tau_{zx}=G\alpha\left(\frac{\partial\phi(x,y)}{\partial x}-y\right),\end{aligned}\tag{4}$$

where G is the shear modulus. If the body force is zero, the equilibrium equations are

$$\begin{aligned}&\frac{\partial\sigma_x}{\partial x}+\frac{\partial\tau_{xy}}{\partial y}+\frac{\partial\tau_{zx}}{\partial z}=0,\\&\frac{\partial\tau_{xy}}{\partial x}+\frac{\partial\sigma_y}{\partial y}+\frac{\partial\tau_{yz}}{\partial z}=0,\\&\frac{\partial\tau_{zx}}{\partial x}+\frac{\partial\tau_{yz}}{\partial y}+\frac{\partial\sigma_z}{\partial z}=0.\end{aligned}\tag{5}$$

By substituting Eq.(4) into Eq.(5), we can find the governing equation as shown below

$$\nabla^2\phi(x,y)=0,\qquad (x,y)\in\Omega,\tag{6}$$

where ∇^2 is the Laplacian operator and Ω is the domain of interest. Since there is no traction on the surface of bar (traction free), the traction in direction z (t_z) must be zero. Thus

$$t_z=\tau_{zx}n_x+\tau_{yz}n_y=0,\qquad (x,y)\in\partial\Omega.\tag{7}$$

By substituting Eq.(4) into Eq.(7), the boundary condition is

$$\frac{\partial\phi}{\partial x}n_x+\frac{\partial\phi}{\partial y}n_y=yn_x-xn_y=\frac{\partial\phi}{\partial n},\qquad (x,y)\in\partial\Omega.\tag{8}$$

Accordingly, the solution of the torsion problem in the form of the warping function with Neumann boundary condition as follows

$$\begin{aligned}&\nabla^2\phi(x,y)=0,\qquad (x,y)\in\Omega,\\&\frac{\partial\phi(x,y)}{\partial n}=yn_x-xn_y,\quad (x,y)\in\partial\Omega.\end{aligned}\tag{9}$$

Since $\phi(x,y)$ is a harmonic function, there exists a function $\varphi(x,y)$ which is relating to $\phi(x,y)$ by the Cauchy-Riemann equations

$$\frac{\partial\phi}{\partial x}=\frac{\partial\varphi}{\partial y},\qquad \frac{\partial\varphi}{\partial x}=-\frac{\partial\phi}{\partial y},\tag{10}$$

where $\varphi(x,y)$ is called the conjugate harmonic function of $\phi(x,y)$. The boundary condition can also be expressed in term of $\varphi(x,y)$ from $\phi(x,y)$ as

$$\begin{aligned}\frac{\partial\phi}{\partial n}&=\frac{\partial\phi}{\partial x}n_x+\frac{\partial\phi}{\partial y}n_y\\&=\frac{\partial\varphi}{\partial y}\frac{dy}{ds}-\frac{\partial\varphi}{\partial x}\frac{dx}{ds}=\frac{d\varphi}{ds}=\frac{1}{2}\frac{d}{ds}\left(x^2+y^2\right),\end{aligned}\tag{11}$$

thus the boundary condition is

$$\varphi(x,y)=\frac{1}{2}\left(x^2+y^2\right)+K,\qquad (x,y)\in\partial\Omega, \tag{12}$$

where K is a constant, it can be set to zero. Therefore, we can obtain a solution of the torsion problem in the form of the conjugate harmonic function with the Dirichlet boundary condition as follows

$$\begin{aligned}\nabla^2\varphi(x,y)&=0, && (x,y)\in\Omega,\\ \varphi(x,y)&=\frac{1}{2}\left(x^2+y^2\right), && (x,y)\in\partial\Omega.\end{aligned} \tag{13}$$

Now we introduce a function $\Phi(x,y)$ relating to $\varphi(x,y)$ by

$$\Phi(x,y)=\varphi(x,y)-\frac{1}{2}\left(x^2+y^2\right). \tag{14}$$

Then, we have

$$\nabla^2\Phi(x,y)=-2,\qquad (x,y)\in\Omega, \tag{15}$$

$$\Phi(x,y)=0,\qquad (x,y)\in\partial\Omega. \tag{16}$$

Since

$$\frac{\partial\Phi}{\partial x}=\frac{\partial\varphi}{\partial x}-x,\qquad \frac{\partial\Phi}{\partial y}=\frac{\partial\varphi}{\partial y}-y, \tag{17}$$

where $\Phi(x,y)$ is the Prandtl function. In this paper, the torsion problem can be formulated as a Poisson equation as given in Eq.(15). The geometric shape of problem is shown in Fig. 3, where a is the length of semi-major axis and b is the length of semi-minor axis. Since Eq.(15) contains the body source term, the governing equation in Eq.(15) and boundary condition in Eq.(16) can be reformulated as

$$\nabla^2\Phi^*(x,y)=0,\qquad (x,y)\in\Omega, \tag{18}$$

$$\Phi^*(x,y)=\frac{x^2+y^2}{2},\qquad (x,y)\in\partial\Omega, \tag{19}$$

where the torsion function $\Phi(x,y)$ can be obtained from $\Phi^*(x,y)$ by superimposing $\widetilde{\Phi}(x,y)$ as follows

$$\Phi^*=\Phi+\widetilde{\Phi}\quad\text{and}\quad \widetilde{\Phi}=\frac{x^2+y^2}{2}. \tag{20}$$

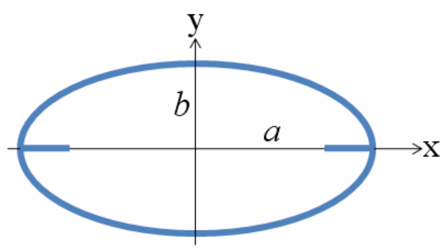

Figure 3 The geometry shape of problem

2.2 Derivation of torsional rigidity

The torsional rigidity C can be determined by

$$\begin{aligned}C&=\frac{M}{\alpha}=\frac{\iint_\Omega\left(x\tau_{yz}-y\tau_{xz}\right)dxdy}{\alpha}\\ &=-G\iint_\Omega\left(x\frac{\partial\Phi}{\partial x}+y\frac{\partial\Phi}{\partial y}\right)dxdy,\end{aligned} \tag{21}$$

where M is the torque, τ_{yz} and τ_{xz} are the shear stresses determined as follows

$$\tau_{yz}=-G\alpha\frac{\partial\Phi}{\partial x},\qquad \tau_{xz}=G\alpha\frac{\partial\Phi}{\partial y}. \tag{22}$$

By employing the Green's second identity and Eq.(15), the area integral in Eq.(21) can be transformed into a boundary integral and an area integral as follows

$$\begin{aligned}C&=-G\iint_\Omega\left(x\frac{\partial\Phi}{\partial x}+y\frac{\partial\Phi}{\partial y}\right)dxdy\\ &=-G\iint_\Omega\left(\nabla\widetilde{\Phi}\cdot\nabla\Phi\right)dxdy\\ &=-G\iint_\Omega\nabla\cdot\left(\widetilde{\Phi}\nabla\Phi\right)dxdy+G\iint_\Omega\widetilde{\Phi}\nabla^2\Phi dxdy\\ &=-G\left(\oint_{\partial\Omega}\widetilde{\Phi}\frac{\partial\Phi}{\partial n}d\partial\Omega+\iint_\Omega\left(x^2+y^2\right)dxdy\right).\end{aligned} \tag{23}$$

The induced area integral of the second term on the right hand side of the equal sign in Eq.(23) can be reformulated into a boundary integral again by using the Gauss theorem as follows

$$\begin{aligned}\iint_A\left(x^2+y^2\right)dxdy&=\frac{1}{16}\iint_\Omega\nabla^2\left\{\left(x^2+y^2\right)^2\right\}dxdy\\ &=\frac{1}{16}\oint_{\partial\Omega}\nabla\left\{\left(x^2+y^2\right)^2\right\}\cdot n d\partial\Omega.\end{aligned} \tag{24}$$

Then the formula of torsional rigidity in a form of boundary integral can be shown as

$$C=-G\oint_{\partial\Omega}\widetilde{\Phi}\frac{\partial\Phi}{\partial n}dB-\frac{G}{16}\oint_{\partial\Omega}\nabla\left\{\left(x^2+y^2\right)^2\right\}\cdot n d\partial\Omega. \tag{25}$$

3. METHOD OF SOLUTION

3.1 Dual boundary element method

By using the Green's identity, the singular boundary integral equation for the domain point x can be derived as follows

$$\begin{aligned}2\pi\Phi^*(x)&=\int_{\partial\Omega}T(s,x)\Phi^*(s)d\partial\Omega(s)\\ &\quad-\int_{\partial\Omega}U(s,x)\frac{\partial\Phi^*(s)}{\partial n_s}d\partial\Omega(s),\qquad x\in\Omega,\end{aligned} \tag{26}$$

where

$$U(s,x)=ln(r), \tag{27}$$

$$T(s,x)=\frac{\partial U(s,x)}{\partial n_s}, \tag{28}$$

in which r is the distance between the field point x and the source point s. After taking the normal derivative from Eq.(26), the hypersingular boundary integral equation for the domain point x can be derived

$$2\pi\frac{\partial\Phi^*(x)}{\partial n_x} = \int_{\partial\Omega} M(s,x)\Phi^*(s)d\partial\Omega(s) - \int_{\partial\Omega} L(s,x)\frac{\partial\Phi^*(s)}{\partial n_s}d\partial\Omega(s), \quad x\in\Omega, \tag{29}$$

where

$$L(s,x)=\frac{\partial U(s,x)}{\partial n_x}, \tag{30}$$

$$M(s,x)=\frac{\partial^2 U(s,x)}{\partial n_x \partial n_s}, \tag{31}$$

in which n_x is the normal vector for the field point x. Eq.(26) and Eq.(29) are termed dual boundary integral equation for the domain point x. The explicit form of the kernel functions can be found in [14]. By tracing the field point x to the boundary, the singular and hypersingular boundary integral equations for the boundary point x can be derived

$$\pi\Phi^*(x) = C.P.V.\int_{\partial\Omega} T(s,x)\Phi^*(s)d\partial\Omega(s) - R.P.V.\int_{\partial\Omega} U(s,x)\frac{\partial\Phi^*(s)}{\partial n_s}d\partial\Omega(s), \quad x\in\partial\Omega, \tag{32}$$

$$\pi\frac{\partial\Phi^*(x)}{\partial n_x} = H.P.V.\int_{\partial\Omega} M(s,x)\Phi^*(s)d\partial\Omega(s) - C.P.V.\int_{\partial\Omega} L(s,x)\frac{\partial\Phi^*(s)}{\partial n_s}d\partial\Omega(s), \quad x\in\partial\Omega, \tag{33}$$

where *R.P.V.* is the Riemann principal value, *C.P.V.* is the Cauchy principal value and *H.P.V.* denote the Hadamard principal value. The boundary integral equations in Eq.(32) and Eq.(33) can be discretized by using constant elements, and the linear algebraic system can be obtained as

$$[T_{ij}]\{\Phi^*\}_j = [U_{ij}]\{\frac{\partial\Phi^*}{\partial n}\}_j, \tag{34}$$

$$[M_{ij}]\{\Phi^*\}_j = [L_{ij}]\{\frac{\partial\Phi^*}{\partial n}\}_j, \tag{35}$$

where [ ] denotes a square influence matrix, { } is a column vector and the elements of the square matrices are

$$U_{ij} = R.P.V.\int U(s_j,x_i)dB(s_j), \tag{36}$$

$$T_{ij} = -\pi\delta_{ij} + C.P.V.\int T(s_j,x_i)dB(s_j), \tag{37}$$

$$L_{ij} = \pi\delta_{ij} + C.P.V.\int L(s_j,x_i)dB(s_j), \tag{38}$$

$$M_{ij} = H.P.V.\int M(s_j,x_i)dB(s_j). \tag{39}$$

4. DERIVATION OF THE MECHANISM OF DEGENERATE BOUNDARY

In the above analysis, we find that the degenerate boundary stems from a singular influence matrix. The degenerate boundary mode and the rigid-body mode will be studied mathematically and numerically in this paper**.**

4.1 Degenerate boundary mode

The equation $[H]\{u\}=\{f\}$ has a unique solution if and only if the only continuous solution to the homogeneous equation

$$[H]\{u\}=\{0\} \tag{40}$$

is $\{u\}=\{0\}$. Alternatively, the homogeneous equation has at least one solution if the homogeneous adjoint equation

$$[H]^\dagger\{\phi\}=\{0\} \tag{41}$$

has a nontrivial solution $\{\phi\}$, where $[H]^\dagger$ is the transpose conjugate matrix of $[H]$ and $\{\phi\}$ must satisfy the constraint $\left(\{f\}^\dagger\{\phi\}=0\right)$. If the matrix $[H]$ is real, the transpose conjugate of a matrix is equal to transpose only, i.e., $[H]^\dagger=[H]^T$. By using the *UT* formulation, we have

$$[U]\{t\}=[T]\{u\}=\{f\}. \tag{42}$$

According to the Fredholm alternative theorem, Eq. (42) has at least one solution for $\{t\}$ if the homogeneous adjoint equation

$$[U]^T\{\phi_1\}=\{0\} \tag{43}$$

has a nontrivial solution $\{\phi_1\}$, in which the constraint $\left(f^T\phi_1=0\right)$ must be satisfied. By substituting Eq.(40) to $\{f\}^T\{\phi\}_1=0$, we obtain

$$[u]^T[T]^T\{\phi_1\}=\{0\}. \tag{44}$$

since $\{u\}$ is an arbitrary vector for the Dirichlet problem, we have

$$[T]^T\{\phi_1\}=\{0\}. \tag{45}$$

Based on Eq.(43) and Eq.(45), we have

$$\begin{bmatrix}[U]^T\\ [T]^T\end{bmatrix}\{\phi_1\}=\{0\} \quad or \quad \{\phi_1\}^T\left[[U] \quad [T]\right]=\{0\}. \tag{46}$$

where Eq.(46) indicates that there is a common left unitary vector in both [*U*] and [*T*] matrices from concept of the SVD updating document.

4.2 Rigid-body mode

Since a rigid body motion is imbedded in the Neuman problem, we have

$$[T]\begin{Bmatrix}1\\ \vdots\\ 1\end{Bmatrix}=0, \tag{47}$$

$$[M]\begin{Bmatrix}1\\ \vdots\\ 1\end{Bmatrix}=0, \tag{48}$$

where Eq.(47) and Eq.(48) reveal that [T] and [M] have common right unitary vector of $\{1....1\}^T$ for the zero singular value.

5. NUMERICAL EXAMPLES

5.1 Dual BEM for determination of torsional rigidity

In this section, the case is designed to examine the accuracy of the dual BEM. Here we use 994 boundary elements to discretize the boundary. There are 200 elements on a single-edge crack, and 594 elements are distributed on the elliptic boundary. Different ratios between minor and major axes, b/a=1/4, 1/2 and 3/4, are considered. Our results are compared with the analytical solution derived by Lebedev et.al. [23]. The analytical formula of torsional rigidity C_a is given below:

$$\frac{C_a}{C_0}=\frac{1+\left(b^2/a^2\right)}{b/a}\left[\frac{32}{\pi^2}\left(1-\frac{b^2}{a^2}\right)Q-\frac{b}{2a}\right], \tag{49}$$

$$Q=\sum_{n=0}^{\infty}\frac{\left[\frac{(2n-1)\sinh(2n+3)\alpha_0+(2n+3)\sinh(2n-1)\alpha_0}{2(2n+1)}-\sinh(2n+1)\alpha_0\right]}{\left(1-4n^2\right)(2n-1)(2n+3)^2\cosh(2n+1)\alpha_0}, \tag{50}$$

$$\alpha_0=\tanh^{-1}\frac{b}{a}, \tag{51}$$

and C_a is the analytical solution of torsional rigidity for an elliptic bar with a double edge crack extending to its foci, C_0 is torsional rigidity of single elliptic bar without crack, a and b are the semi-axes of the ellipse. The analytical torsional rigidity of an elliptic bar without a crack is

$$C_0=G\frac{\pi a^3b^3}{a^2+b^2}. \tag{52}$$

The numerical solutions are shown in Table 1. The relative error of the numerical solution decreases by increasing the number of element as shown in Fig. 4.

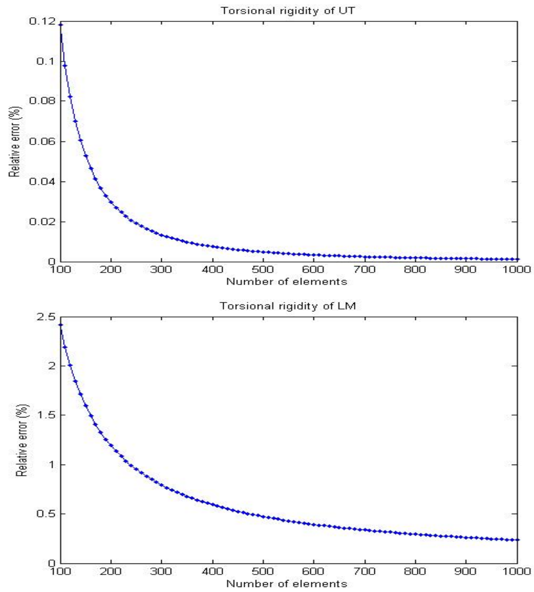

Figure 4 Relative errors by using the UT/LM approach versus number of elements

5.2 Singular value decomposition technique

By employing the singular value decomposition (SVD) to the four influence matrices in the dual BEM ([U]、[T]、[L] and [M]), the information of physics and mathematics can be found in the right and left unitary vectors. We consider an elliptic torsion bar containing a degenerate boundary (e.g. crack) as shown in Table 2. The rank of matrices [U] and [L] is deficient due to the degenerate boundary, and the rank of matrices [T] and [M] is deficient due to both the degenerate boundary and rigid body motion. By using the SVD technique, the four influence matrices [U], [T], [L] and [M] can be decomposed as

$$\begin{aligned}[U]&=\left[\Phi^U\right]\left[\Sigma^U\right]\left[\Psi^U\right]^T,\\ [T]&=\left[\Phi^T\right]\left[\Sigma^T\right]\left[\Psi^T\right]^T,\\ [L]&=\left[\Phi^L\right]\left[\Sigma^L\right]\left[\Psi^L\right]^T,\\ [M]&=\left[\Phi^M\right]\left[\Sigma^M\right]\left[\Psi^M\right]^T.\end{aligned} \tag{53}$$

Table 1 Torsional rigidity for cases of three different ratios (*b*/*a*=1/4, 1/2 and 3/4)

Item \ $\frac{b}{a}$	$\frac{1}{4}$	$\frac{1}{2}$	$\frac{3}{4}$
Analytical solution Eq.(49)	11.8155	4.8758	179.3633
DBEM UT-approach	11.8137	4.8882	179.1036
DBEM LM-approach	11.2511	4.8653	178.8932
Error-UT (%)	0.0001	0.0001	0.0006
Error-LM (%)	0.0478	0.0046	0.0005

We consider a simple problem containing a degenerate boundary as shown in Table 2. We plot the right and left unitary vectors of [*U*] corresponding to the zero singular value in a bar chart as shown in Fig. 5, where matrix [*U*] contains two zero singular values caused by degenerate boundary and matrix [*T*] contains three zero singular values that include two due to degenerate boundary and one due to rigid-body mode. In the same way, we plot the bar chart of all four influence matrices [*U*], [*T*], [*L*] and [*M*]. The bar charts are shown in Fig. 6, and Fig. 7 shows the bar charts after superposing the unitary vector corresponding zero singular values. Hence, we found that the same fictitious information of mathematics comes from the degenerate boundary and the same true information of physics stems from the rigid body motion as shown in Fig. 8. We also present a more complex case which has 214 elements as shown in Fig. 9, and it shows the same result as the case of 10 elements.

Table 2 Rank of four influence matrices (10 elements)

Type of BEM \ Rank of matrix	[*U*]	[*T*]	[*L*]	[*M*]
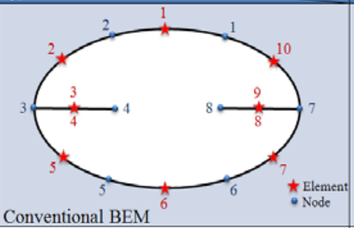 Conventional BEM	8	7	8	7
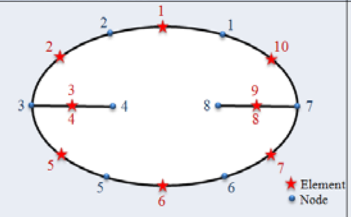 Dual BEM [*U*] ↔ [*L*] [*T*] ↔ [*M*]	10	9	10	9

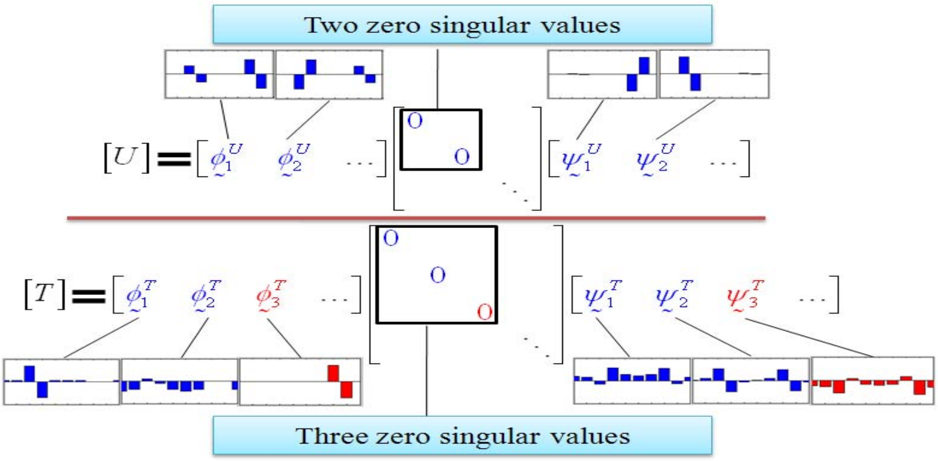

Figure 5 Unitary vectors of [*U*] (two zero singular values) and [*T*] (three zero singular values) in bar charts

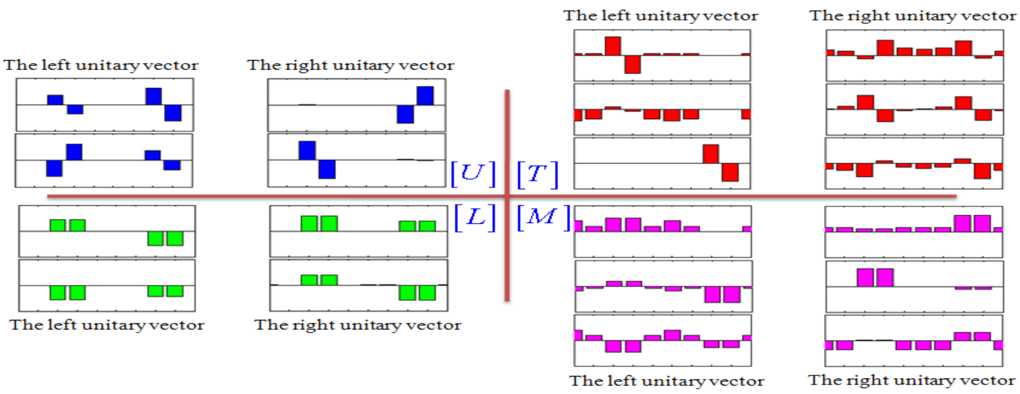

Figure 6 Bar charts of the right and left unitary vectors of [*U*], [*T*], [*L*] and [*M*]

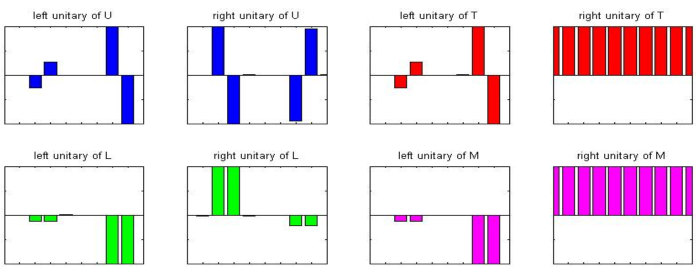

Figure 7 Bar charts of the right and left unitary vectors (10 elements)

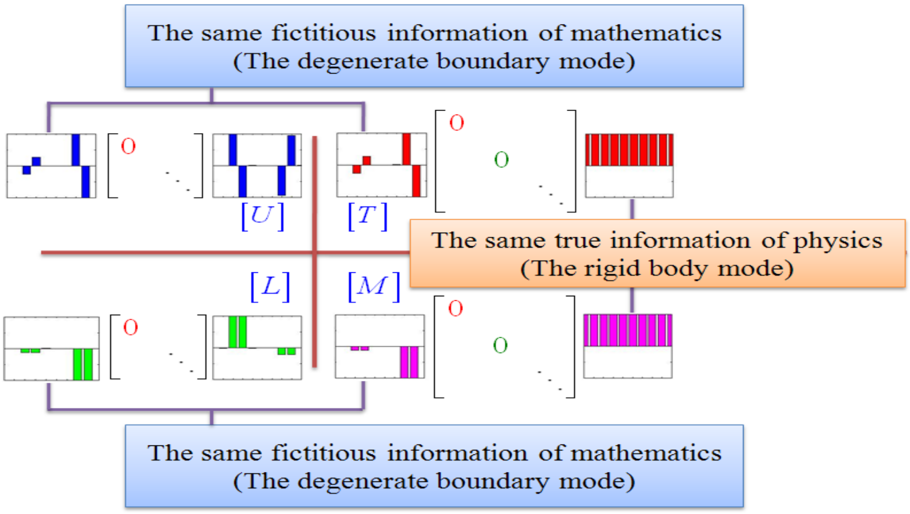

Figure 8 Relation of each matrix (10 elements)

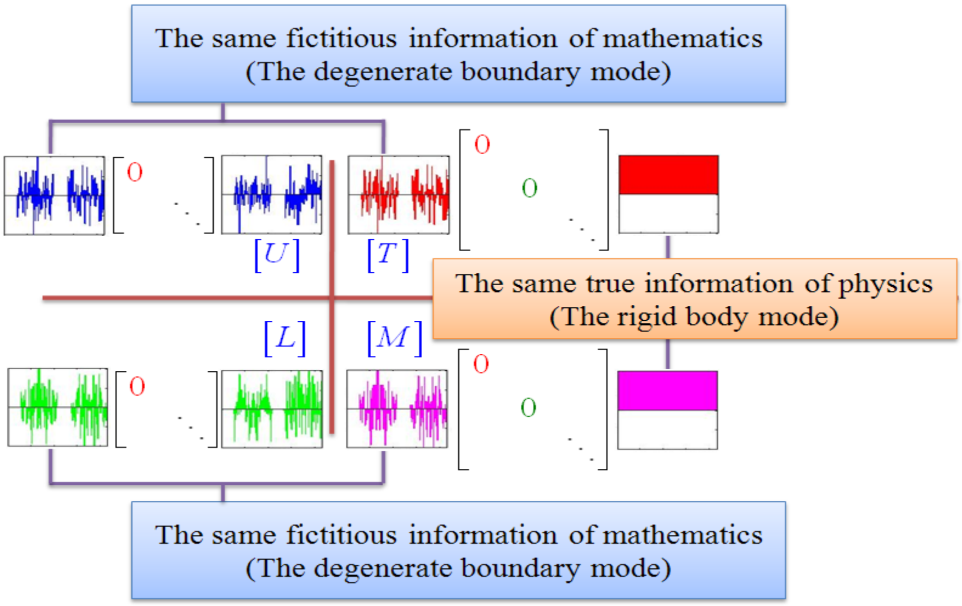

Figure 9 Relation of each matrix (214 elements)

6. CONCLUSIONS

The dual boundary element method was applied to solve torsion problem of an elliptic bar containing a double-edge crack. The results show that the dual BEM has high accuracy. The dual BEM involves modeling only on the boundary in a single domain free of introducing the artificial boundary in the multi-domain method. The results have been compared with analytical solutions well. By employing the singular value decomposition technique to the four influence matrices, the degenerate boundary contributes the rank deficiency in the common left unitary vector of the [*U*] and [*T*] matrices. Rigid body modes are imbedded in the common right unitary vector of [*L*] and [*M*] matrices. The reason why dual BEM can solve the crack problem is well understood in this paper.

7. ACKNOWLEDGEMENT

Financial support from the National Science Council under Grant No. NSC 100-2221-E-019-040-MY3 for National Taiwan Ocean University is gratefully acknowledged.

8. REFERENCES

[1] N. Kinoshita and T. Mura, “On boundary value problem of elasticity,” Research Report of the Faculty of Engineering, Meiji Univ., No.8, pp. 56-82, 1956.

[2] F.J. Rizzo, “An integral equation approach to boundary value problems of classical elastostatics,” *Quarterly Appl., Math.*, 25, pp. 83- 95, 1967.

[3] G.E. Blandford, A.R. Ingraffea and J.A. Liggett, “Two-dimensional stress intensity factor computations using the boundary element method,” *Int. J. Num. Meth. Eng.*, 17, pp. 387- 404, 1981.

[4] H-K. Hong and J.T. Chen, "Derivation of integral equations in elasticity," *J. Eng. Meth. Div., ASCE*, Vol. 114, No. 6, Em5, pp. 1028- 1044, 1988.
[5] J.T. Chen, "On Hadamard principal value and boundary integral formulation of fracture mechanics," Master Thesis, Institute of Applied Mechanics, National Taiwan University, 1986.
[6] A. Portela, M.H. Aliabadi and D.P. Rooke, "The dual boundary element method: effective implementation for crack problems," *Int. J. Num. Meth. Eng.*, Vol. 33, pp. 1269- 1287, 1992.
[7] P. Fedelinski and M.H. Aliabadi, "The dual boundary element method: J-integral for dynamic stress intensity factors," *Int. J. Fracture*, Vol. 65, No. 4, pp. 369- 381, 1994.
[8] V. Leitao, M.H. Aliabadi and D.P. Rooke, "The boundary element formulation for elastoplastic fracture mechanics," *Int. J. Num. Meth. Eng*, Vol. 38, pp. 315- 333, 1995.
[9] O.E. Lafe, J.S. Montes, A.H.D. Cheng, J.A. Liggett and P.L.-F. Liu, "Singularity in Darcy flow through porous media," *J. Hydraul. Div., ASCE*, 106 (HY6), pp. 977- 997, 1980.
[10] J.T. Chen and H-K. Hong, "On the dual integral representation of boundary value problem in Laplace equation," *Boundary Element Abstracts*, Vol. 4, No. 3, pp. 114- 116, 1993.
[11] J.T. Chen, H-K. Hong and S.W. Chyuan, "Boundary element analysis and design in seepage flow problems with sheet piles," *Finite Element in Analysis and Design*, Vol. 17, pp. 1- 20, 1994.
[12] P.L.-F. Liu and M. Abbaspour, "Wave scattering by a rigid thin barrier," *J. Waterway Port Coast. Ocean Div., ASCS*, 108 (WW4), pp. 479- 487, 1982.
[13] C.S. Wang, S. Chu and J.T. Chen, "Boundary element method for predicting store airloads during its carriage and separation procedures," *Computational Engineering with Boundary Elements*, Vol. 1, Fluid and Potential Problems, pp. 305- 317, 1990.
[14] J.T. Chen and H-K. Hong, "Boundary Element Method," New World Press, Taipei, 1992. (in Chinese)
[15] H-K. Hong and J.T. Chen, "Generality and special cases of dual integral equations of elasticity," *J. Chinese Soc. Mech. Eng.*, 9, pp. 1- 19, 1988.
[16] J.T. Chen, K.H. Chen and W. Yeih, "Dual boundary element analysis for cracked bars under torsion," *Engineering Computations*, Vol. 15, No. 6, pp. 732- 749, 1998.
[17] J.T. Chen and Y.W. Chen, "Dual boundary elements analysis using complex variables for potential problems with or without a degenerate boundary," *Engineering Analysis with Boundary Elements*, Vol. 24, pp. 671- 684, 2000.
[18] J.T. Chen, W.C. Shen and P.Y. Chen, "Analysis of Circular Torsion Bar with Circular Holes Using Null-field Approach," *Computer Modelling in Engineering Science*, Vol. 12, No. 2, pp. 109- 119, 2006.
[19] J.T. Chen and Y.T. Lee, "Torsional rigidity of a circular bar with multiple circular inclusions using the null-field integral approach," *Computational Mechanics*, Vol. 44, pp. 221- 232, 2009.
[20] J.T. Chen, Y.T. Lee and J.W. Lee, "Torsional rigidity of an elliptic bar with multiple elliptic inclusions using a null-field integral approach," *Computational Mechanics*, Vol. 46, pp. 511- 519, 2010.
[21] Y. Mi. and M.H. Aliabadi, "Dual boundary element method for three dimensional fracture mechanics analysis," *Engineering Analysis with boundary Elements*, Vol. 10, No. 2, pp. 161- 171, 1992.
[22] J.T. Chen, C.F. Lee and S.Y. Lin, "A new point of view for the polar decomposition using singular value decomposition," *International Journal of Computational and Numerical Analysis and Applications*, Vol. 2, No. 3, pp. 257- 264, 2002.
[23] N.N. Lebedev, I.P. Skalskaya and Y.S. "Worked problems in applied mathematics," Dover, pp. 203- 210, 1965.
[24] A.P. Boresi and K.P. Chong, "Elasticity in engineering mechanics," A Wiley-Interscience Publication.

含雙邊裂縫橢圓桿扭轉之對偶邊界元素法分析

范　羽[1]、李應德[1]、李家瑋[1]、陳正宗[1, 2]

[1]國立臺灣海洋大學河海工程學系

[2]國立臺灣海洋大學機械與機電工程學系

摘要

眾所皆知邊界元素法在處理含有退化邊界(如裂縫)的問題時會遇到矩陣秩降的行為，這也是為什麼用傳統邊界元素法時必須將問題切割成多領域後才能求解的原因。因此，將超奇異積分方程式引入使解唯一，就能避免秩降發生於含有退化邊界的問題且不需將領域分割。其中，四個影響係數矩陣有著對偶的架構，所以稱此為對偶邊界元素法。藉由使用奇異值分解法將四個影響係數矩陣作分析，可發現其中蘊含之數學與物理機制。其中，真實的物理秩降現象會在影響係數矩陣中零奇異值所對應的右酉向量中反映出剛體運動的行為，而退化邊界所造成虛擬的數學秩降現象則出現在影響係數矩陣中零奇異值所對應的左酉向量中。本文中，我們將使用對偶邊界元素法來計算含雙邊裂縫橢圓桿的扭轉剛度。最後，本文也會針對奇異值分解中右酉與左酉向量所發生的現象做詳細的討論。

關鍵詞：退化邊界、對偶邊界元素法、零場積分方程式、奇異值分解法、扭轉剛度。